

Electronic structure of titanium. III

R. M. Welch and E. H. Hygh

Department of Physics, University of Utah, Salt Lake City, Utah 84112

(Received 3 April 1973)

The band structure and Fermi surface of titanium have been calculated using the augmented-plane-wave method. The present calculation, carried out using a potential that is derived from the atomic configuration $3d^3 4s^1$, is compared with previous results obtained by using the configuration $3d^2 4s^2$.

I. INTRODUCTION

The present paper reports the results of an augmented-plane-wave (APW) calculation of the electronic energy-band structure of titanium using the atomic configuration $3d^3 4s^1$ with full exchange. Previous results using the atomic configuration $3d^2 4s^2$ and full exchange have been reported in an earlier paper¹ [HW(I)]. A self-consistent APW calculation using $\frac{3}{4}$ instead of full exchange has been reported² [WH(II)].

The results of recent de Haas-van Alphen measurements by Kamm³ disagree with previous results^{1,2} of theoretical Fermi-surface calculations. Results from an APW calculation by Mattheiss⁴ using configuration $3d^3 4s^1$, seem to compare quite well with the experimental data.³ However, only the energy bands from Γ to K [see Fig. 1(b)] in the Brillouin zone (BZ) have been calculated by Mattheiss. Therefore, we have decided to complete the calculation with the hope of obtaining better agreement with the experimental data.

II. DETAILS OF CALCULATION

Titanium has the hcp crystal structure [see Fig. 1(a)] with lattice constants $a = 5.5769$ a. u. and $c = 8.8523$ a. u. The dimensions of the BZ [see Fig. 1(b)] are $\Gamma A = 0.3549$ (a. u.)⁻¹, $\Gamma K = 0.751$ (a. u.)⁻¹, and $\Gamma M = 0.650$ (a. u.)⁻¹. The basis vectors for the direct and reciprocal lattice are given by

$$\begin{aligned} \bar{a}_1 &= c\hat{z}, \quad \bar{a}_2 = a\hat{x}, \quad \bar{a}_3 = -\frac{1}{2}a\hat{x} + \frac{1}{2}\sqrt{3}a\hat{y}, \\ \bar{b}_1 &= \frac{1}{c}\hat{z}, \quad \bar{b}_2 = \frac{1}{a}\hat{x} + \frac{1}{\sqrt{3}a}\hat{y}, \quad \bar{b}_3 = \frac{2}{\sqrt{3}a}\hat{y}. \end{aligned}$$

The reciprocal-lattice vectors used in the APW expansion are designated by

$$\bar{g} = (n_1, n_2, n_3) = 2\pi(n_1\bar{b}_1 + n_2\bar{b}_2 + n_3\bar{b}_3).$$

The calculation was carried out over a discrete mesh which is equivalent to 7670 points in the BZ. Eigenvalues were calculated at each of the 45 points on each of the 9 levels as shown in Fig. 2, using APW's defined by the 35 reciprocal-lattice vectors shown in Table I. Group theory was used

for the calculations along high-symmetry directions in order to simplify the calculation [see WH(II)].

III. RESULTS

The energy bands shown in Fig. 3 are similar to those obtained in HW(I) and WH(II). The energy of the highest occupied state was found to be 0.401 Ry. The energy of the lowest state at Γ was 0.124 Ry, which gives an occupied bandwidth of 0.277 Ry.

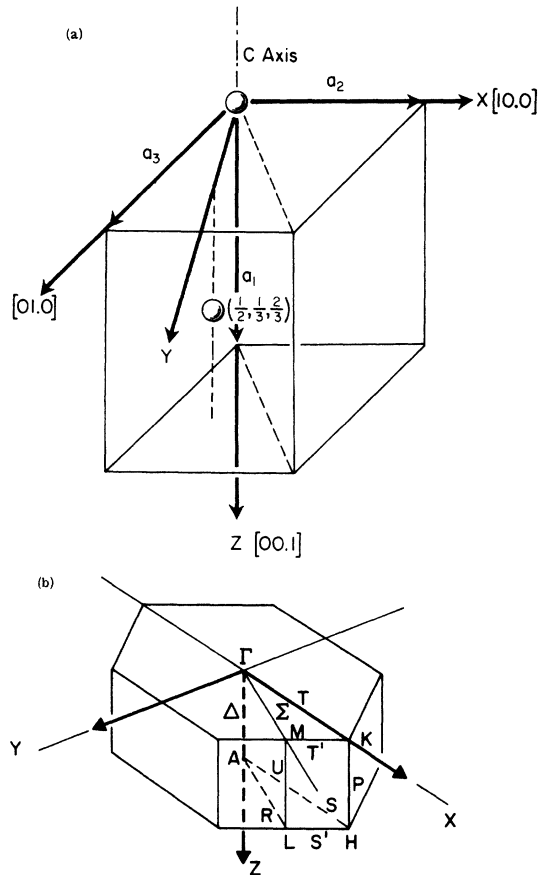


FIG. 1. (a) Unit cell for the hexagonal-close-packed crystal structure. (b) Half of the Brillouin zone for the hexagonal-close-packed structure with the $\frac{1}{24}$ th zone.

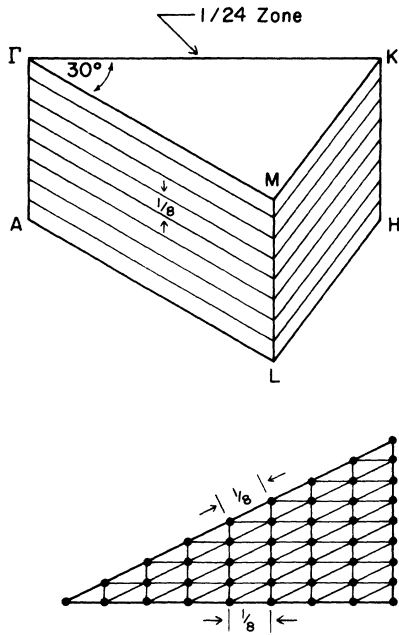


FIG. 2. The $\frac{1}{24}$ th zone showing the calculation mesh.

As before, the double-zone scheme is used to display connections of the Fermi surface in the third and fourth as well as in the fifth and sixth zones. Intersections of the Fermi surface with the symmetry planes of the $\frac{1}{24}$ double-zone wedge are shown in Fig. 4(a) for the third and fourth

TABLE I. Reciprocal-lattice vectors used in this study.

$(0, 0, 0)$	$(1, 0, 0)$	$(\bar{1}, 1, 0)$	$(1, \bar{1}, 1)$	$(0, \bar{1}, \bar{1})$	$(0, 1, 2)$	$(\bar{1}, 0, \bar{2})$
$(0, 0, 1)$	$(\bar{1}, 0, 0)$	$(1, 0, 1)$	$(\bar{1}, 1, 1)$	$(1, \bar{1}, \bar{1})$	$(0, \bar{1}, 2)$	$(0, 1, \bar{2})$
$(0, 0, \bar{1})$	$(0, 1, 0)$	$(\bar{1}, 0, 1)$	$(1, 0, \bar{1})$	$(\bar{1}, 1, \bar{1})$	$(1, \bar{1}, 2)$	$(0, \bar{1}, \bar{2})$
$(0, 0, 2)$	$(0, \bar{1}, 0)$	$(0, 1, 1)$	$(\bar{1}, 0, \bar{1})$	$(1, 0, 2)$	$(\bar{1}, 1, 2)$	$(1, \bar{1}, \bar{2})$
$(0, 0, \bar{2})$	$(1, \bar{1}, 0)$	$(0, \bar{1}, 1)$	$(0, 1, \bar{1})$	$(\bar{1}, 0, 2)$	$(1, 0, \bar{2})$	$(\bar{1}, 1, \bar{2})$

zones and are shown in Fig. 4(b) for the fifth and sixth zones. Figure 5 shows the Fermi surface in the double-zone scheme for the third and fourth zones. Likewise, Fig. 6 shows the Fermi surface for the fifth and sixth zones. The shaded portions of Figs. 5 and 6 are hole and electron surfaces, respectively.

IV. DISCUSSION

The energy bands shown in Fig. 3 are quite similar to those obtained in HW(I). Each state has been labeled according to symmetry in order to establish the continuity of energy solutions. This was also done in WH(II), but was not done with HW(I). We see that along ΓK the band structure near the Fermi energy is nearly identical to that obtained in HW(I). However, the self-consistent results in WH(II) indicate the band T_1 from Γ_{1+} to K_1 crosses the Fermi energy, whereas the present calculation does not. Along KM and $M\Gamma$ the energy band structure is very similar to the WH (II) results except that the M_1 state is now slightly above the Fermi level. Therefore, the

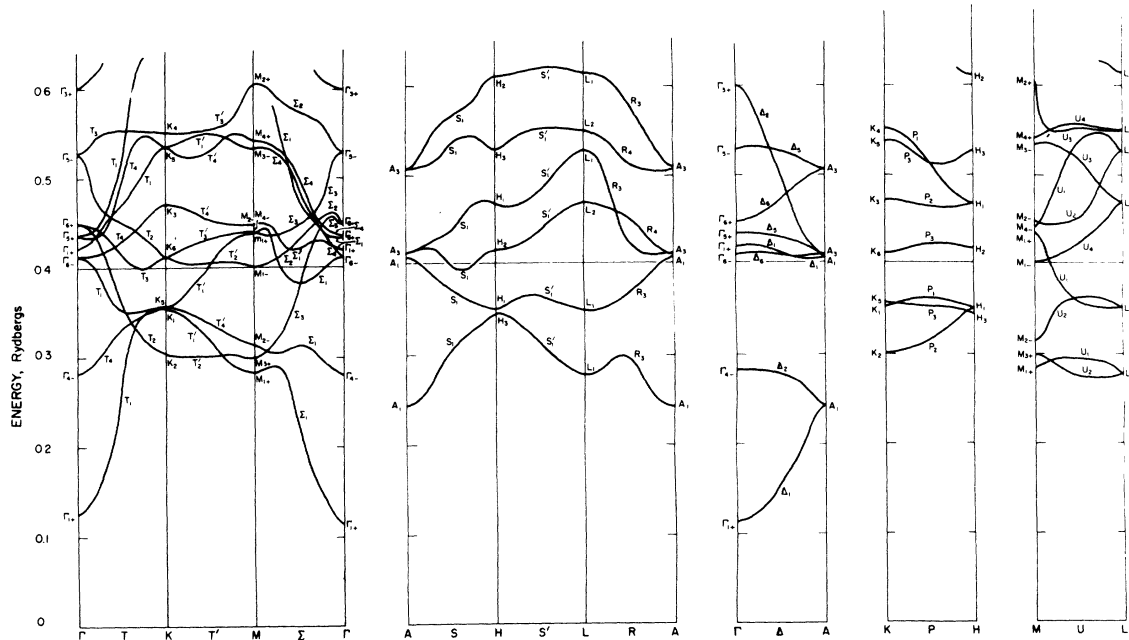


FIG. 3. Energy bands for titanium along symmetry directions.

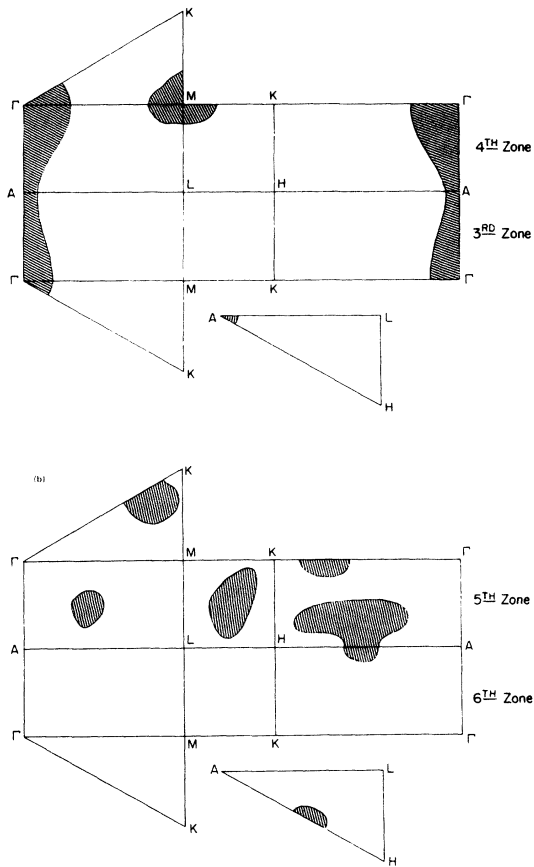


FIG. 4. (a) Intersections of the Fermi surface with the symmetry planes of the double wedge for the third and fourth zones. (b) Intersections of the Fermi surface with the symmetry planes of the double wedge for the fifth and sixth zones.

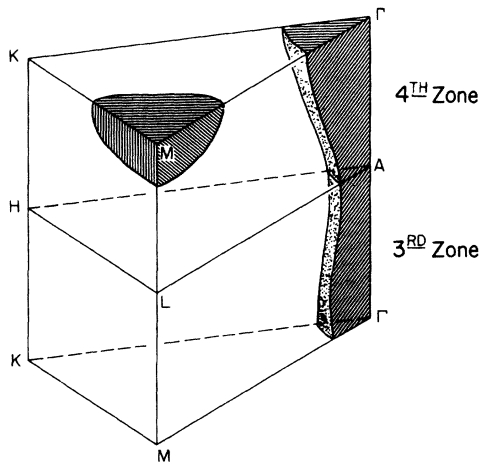


FIG. 5. Fermi surface for the third and fourth zones.

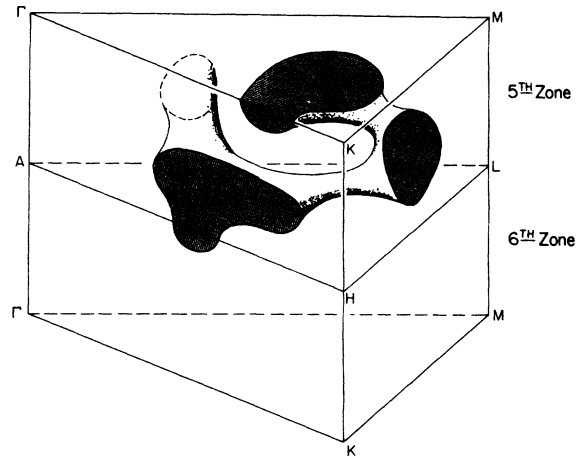


FIG. 6. Fermi surface for the fifth and sixth zones.

fourth band pocket of electrons centered at M no longer appears. The fifth band no longer dips below the Fermi level along KM as was the case in HW(I). The band structure along all other high-symmetry directions is in close agreement with the results obtained in HW(I).

We see that along AH the fifth and sixth bands dip below the Fermi level instead of the third and fourth bands rising above the Fermi energy as was the case in WH(II). In addition, the present results do not show the fourth band rising above the Fermi level between K and H as was the case in WH(II). Therefore, the pockets of holes seen along ΓK , KH , and AH in WH(II) are not predicted by the present calculation. With the above mentioned differences, we see that the third- and fourth-zone band structures are remarkably consistent for all three calculations.

A primary reason for repeating this calculation for titanium was to determine whether or not the hole surface along ΓA in the third and fourth zones becomes disconnected for the change in configuration from $3d^2 4s$ to $3d^3 4s^1$. All three calculations predict a continuous surface in spite of the fact that the experimental results³ indicate a break in this surface near point A .

Comparing the Fermi surface in the fifth and sixth zones we find good agreement with the results for HW(I). The principal difference seems to be that the fifth band crosses the Fermi level along MK in HW(I) but does not in the present results. Also, the electron structures found in the sixth zone and along the symmetry plane ΓKM in the fifth zone are not present in WH(II). In spite of the differences among the three calculations, the major features are preserved. The intersections of the electron surface with the ΓALM , ΓKH , ΓAHK , and $KMLH$ planes still occur

in the fifth zone.

The differences between the present energy bands along ΓK and those obtained by Mattheiss are due to the fact that he used atomic charge densities generated⁴ by Hartree-Fock self-consistent-field (SCF) calculations while our charge densities were the result of Hartree-Fock-Slater SCF calculations carried out by Liberman.⁵

V. CONCLUSIONS

Predictions from all three titanium calculations disagree with experimental de Haas-van Alphen results. It is interesting to observe however that qualitative agreement with experiment for the structure in the third and fourth zones along high-symmetry direction ΓA can be obtained by arbitrarily shifting the Fermi energy up to $E_F = 0.41$ Ry from its calculated value of $E_F = 0.401$ Ry. Under this condition, the third and fourth bands

dip below the Fermi level near high-symmetry point A in agreement with experiment. This kind of shifting of the Fermi energy to fit experimental data was also suggested by Loucks⁶ for zirconium.

The Fermi-surface shape is extremely sensitive to relatively small changes in the value of the Fermi level. Any further refinement in accuracy of the present calculation within the framework of the basic APW method most likely will not bring about the necessary change in the value of the energy required to produce the desired changes in the Fermi surface. In contrast, it was found in WH(II) that the calculated value of the Fermi energy is particularly sensitive to small changes in the potential. As such, a more refined and accurate calculation of exchange potential coupled with a careful determination of both the nonflat and nonspherical corrections to the potential energy may well be the answer.

¹E. H. Hygh and Ronald M. Welch, Phys. Rev. B 1, 2424 (1970).

²Ronald M. Welch and E. H. Hygh, Phys. Rev. B 4, 4261 (1971).

³George Kamm (private communication).

⁴L. F. Mattheiss, Phys. Rev. 134, A970 (1964).

⁵We are grateful to Dr. David Liberman for making available the unpublished results of his Hartree-Fock-Slater self-consistent-field calculations for titanium.

⁶T. L. Loucks, Phys. Rev. 159, 544 (1967).

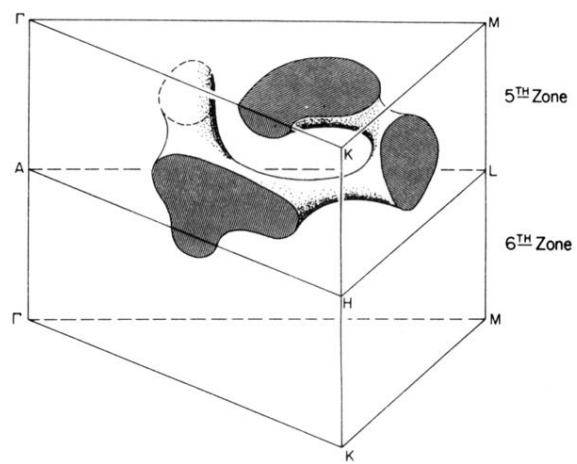


FIG. 6. Fermi surface for the fifth and sixth zones.